JSHC
Japan Society of
Histochemistry and Cytochemistry
Established 1959

Acta Histochem. Cytochem. 47 (2): 59–65, 2014
doi: 10.1267/ahc.14014

Pacing-Induced Non-Uniform Ca^{2+} Dynamics in Rat Atria Revealed by Rapid-Scanning Confocal Microscopy

Yan Jiang[1], Hideo Tanaka[1], Taka-aki Matsuyama[1,2], Yoshihisa Yamaoka[1] and Tetsuro Takamatsu[1]

[1]Department of Pathology and Cell Regulation, Kyoto Prefectural University of Medicine, Graduate School of Medical Science, Kyoto, 602-8566, Japan and [2] Department of Pathology, National Cerebral and Cardiovascular Center, Suita, Osaka 565-8565, Japan

Received February 21, 2014; accepted February 28, 2014; published online April 25, 2014

Intracellular Ca^{2+} ($[Ca^{2+}]_i$) dynamics in isolated myocytes differ between the atria and ventricles due to the distinct t-tubular distributions. Although cellular aspects of ventricular $[Ca^{2+}]_i$ dynamics in the heart have been extensively studied, little is known about those of atrial myocytes *in situ*. Here we visualized precise $[Ca^{2+}]_i$ dynamics of atrial myocytes in Langendorff-perfused rat hearts by rapid-scanning confocal microscopy. Of 16 fluo-4-loaded hearts imaged during pacing up to 4-Hz, five hearts showed spatially uniform Ca^{2+} transients on systole among individual cells, whereas no discernible $[Ca^{2+}]_i$ elevation developed during diastole. In contrast, the remaining hearts showed non-uniform $[Ca^{2+}]_i$ dynamics within and among the cells especially under high-frequency (4 Hz) excitation, where subcellular cluster-like $[Ca^{2+}]_i$ rises or wave-like $[Ca^{2+}]_i$ propagation occurred on excitation. Such $[Ca^{2+}]_i$ inhomogeneity was more pronounced at high-frequency pacing, showing beat-to-beat Ca^{2+} transient alternans. Despite such non-uniform dynamics, cessation of burst pacing of the atria was not followed by emergence of spontaneous Ca^{2+} waves, indicating minor Ca^{2+}-releasing potentials of the sarcoplasmic reticulum (SR). In summary, rat atria display a propensity to show non-uniform $[Ca^{2+}]_i$ dynamics on systole due to impaired Ca^{2+}-release from the SR and paucity of t-tubules. Our results provide an important basis for understanding atrial pathophysiology.

Key words: atrium, Ca^{2+} transient, Ca^{2+} alternans, transverse tubule, rat

I. Introduction

The calcium ion (Ca^{2+}) plays a pivotal role in excitation-contraction coupling of the heart [4]. Given that cardiac performance is determined by electromechanical coordination of individual cardiomyocytes, visualization of the cellular aspects of intracellular Ca^{2+} concentration ($[Ca^{2+}]_i$) dynamics in the heart is an important means of understanding cardiac pathophysiology [24]. So far, studies on $[Ca^{2+}]_i$ dynamics of cardiomyocytes have been well described not only under enzymatically isolated conditions [6, 22] but also in working ventricles [1, 9–13, 18, 20, 23–25]. For example, we have reported cellular $[Ca^{2+}]_i$ dynamics in rat hearts imaged by using *in situ* rapid scanning confocal microscopy [9–12, 23–25]. These studies revealed that individual ventricular myocytes in the intact heart show spatiotemporally uniform $[Ca^{2+}]_i$ on beat-to-beat basis, whereas non-uniform $[Ca^{2+}]_i$ dynamics emerge in diseased or injured hearts, e.g., Ca^{2+} waves that emerge under $[Ca^{2+}]_i$ overload. Furthermore, $[Ca^{2+}]_i$ dynamics under diseased conditions have also been studied in the ventricles, where myocytes show non-uniform $[Ca^{2+}]_i$ dynamics [1, 13]. However, compared with the ventricular $[Ca^{2+}]_i$ dynamics, little is known about the atrial $[Ca^{2+}]_i$ dynamics within the heart. Considering that cellular aspects of $[Ca^{2+}]_i$

Correspondence to: Hideo Tanaka, MD., PhD., Department of Pathology and Cell Regulation, Kyoto Prefectural University of Medicine, Graduate School of Medical Science, Kawaramachi Hirokoji, Kamigyo-Ku, Kyoto 602-8566, Japan. E-mail: hideotan@koto.kpu-m.ac.jp

dynamics of isolated atrial myocytes are different from those of ventricular cells due to the poorly developed transverse tubules (t-tubules) as compared with those in ventricular myocytes [2, 21], there is a possibility that atrial myocytes exhibit distinct cellular aspects of $[Ca^{2+}]_i$ dynamics within the working atria. So far, there is only one report, recently published, on $[Ca^{2+}]_i$ dynamics in excised mouse hearts with genetic mutation of Ca^{2+}-releasing channels, ryanodine receptors in the sarcoplasmic reticulum (SR), where the atrial myocytes were found to exhibit spatiotemporally non-uniform $[Ca^{2+}]_i$ dynamics that may relate to genesis of atrial tachyarrhythmias [26]. Nevertheless, still unknown is precise intracellular behaviors of $[Ca^{2+}]_i$ in intact atria, particularly whether and how spatial uniformity of $[Ca^{2+}]_i$ dynamics is altered on the basis of intrinsic structural features. To address these unresolved issues, we sought to visualize and quantitatively analyze detailed $[Ca^{2+}]_i$ dynamics of the atrial myocytes in Langenforff-perfused rat hearts by using rapid scanning confocal microscopy. Our present study provides an important basis for understanding pathophysiology of the atrium.

II. Materials and Methods

Sixteen adult Wistar rats weighing 250–300 g were used. The rats were treated in accordance with *The Guide for the Care and Use of Laboratory Animals* published by the US National Institutes of Health (NIH publication No. 85 to 23, revised 1985), and with the approval of the Animal Care Committee at Kyoto Prefectural University of Medicine. The heart was excised under anesthesia by intraabdominal injection of pentobarbital sodium (0.1 mg/g of body weight), and perfused in a Langendorff manner for 5 min with a 1 mM Ca^{2+}-containing Tyrode's solution consisting of (in mM) NaCl 145, KCl 5.4, $MgCl_2$ 1, HEPES 10, and glucose 10 (pH=7.4 adjusted by NaOH) at 23–25°C. Washout of the blood was followed by loading of the heart with a Ca^{2+} indicator, fluo 4-AM (8 μg/ml, Dojindo). After 30-min loading of fluo-4, the heart was perfused with the Tyrode's solution at 37°C for 5 min for de-esterification of the AM form of the probe with probenecid (0.1 mg/ml) added, and served for experiments. Under placement of the heart on an upright microscope (BX-50WI, Olympus) covered with a glass coverslip (170-μm thickness), the subepicardial surface of the atrial appendage of either side was excited by a 488-nm argon laser (Melles Griot) and emitted fluorescence (peak wavelength, ~530 nm) visualized by a rapid scanning confocal microscope equipped with a spinning disc-type confocal unit CSU-21 (Yokogawa) as described previously [9, 11, 23] at a frame rate of 33.3/s. During experiments the heart was under constant perfusion with Krebs-Henseleit solution containing (in mM) NaCl 115, $NaHCO_3$ 25, KCl 5.4, NaH_2PO_4 1.2, $NaHCO_3$ 25, $MgSO_4$ 1, $CaCl_2$ 1, and glucose 10, aerated with 95% O_2 and 5% CO_2, flowing at 10 ml/min at room temperature (~25°C). Cytochalasin D (4 μM) was added to the perfusate to suppress mechanical motion. The emitted fluorescent signals were detected through an image intensifier (C8600, Hamamatsu Photonics) by a CCD camera (MiCaM02, Brainvision) with a pixel size of 384×256 pixels (361×241 μm) via a 20× objective lens (UMPLan FI, NA 0.5, Olympus). Waveforms of Ca^{2+} transients were quantified by measuring the amplitude and duration at 20%, 50% and 70% decays of the transients. Morphology of the atria was imaged after staining of the sarcolemmal membrane with coronary perfusion and immersion of a membrane dye di-4-ANEPPS (0.1 μg/ml) in 20 ml Tyrode's solution. Besides the $[Ca^{2+}]_i$ imaging, fluorescence imaging was conducted of the di-4-ANEPPS-stained hearts (n=3) by excitation of a 488-nm argon laser on the subepicardial surface of bilateral atrial appendages and the left ventricular free wall by using an FV1000 confocal microscope (Olympus). Electrical activities were simultaneously recorded under image detection by using a MiCaM02 data acquisition system via bipolar Ag-AgCl wire electrodes located on either side of the heart. The atria were electrically paced via bipolar Ag-AgCl electrodes by an electrical stimulator (SEN-3301, Nihon Kohden) at rates ranging from 1 Hz to 4 Hz. Fluorescence images were analyzed by using Image J software (NIH). Quantitative data are shown as mean±SD, and statistical significance of the data was evaluated by Student's t test with a p value of <0.05 regarded denoting significant difference.

III. Results

To elucidate the structural basis of the atrial myocytes within the atrial appendages in the rat heart, we conducted confocal imaging of these tissues stained with the membrane dye di-4ANEPPS (Fig. 1). It was found that atrial myocytes delineated by the ANEPPS-fluorescence are thinner than ventricular myocytes. Close observations of the individual cells revealed that ventricular myocytes showed fine networks of t-tubules in overall cells, whereas atrial myocytes were often lacking in the tubular structures.

In five hearts out of 16 examined, fluo-4-loaded atrial myocytes exhibited spatially uniform $[Ca^{2+}]_i$ dynamics in individual atrial myocytes of the left atrial appendage on excitation as evidenced by representative X-t images under consecutive atrial pacing at 1 to 4 Hz (Fig. 2A). On the other hand, no discernible rise of $[Ca^{2+}]_i$ occurred in between the Ca^{2+} transients (i.e., during diastole), indicating absence of $[Ca^{2+}]_i$ overload in the atria. The corresponding plot profiles of fluo-4 fluorescence revealed that the configuration of the Ca^{2+} transient was uniform during the constant-frequency pacing. Quantitatively, the duration of Ca^{2+} transient was excitation-frequency dependent. Pooled data from five hearts revealed that Ca^{2+} transients are abbreviated in accordance with the frequency of pacing (Fig. 2B-a). During consecutive pacing, both the amplitude and duration of Ca^{2+} transients were nearly constant, albeit a small variability in these parameters develops during 4-

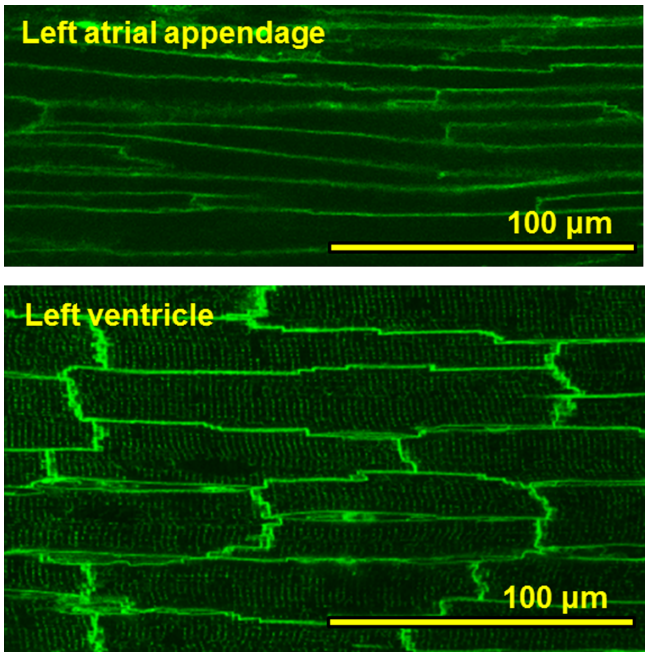

Fig. 1. Confocal images of cell structures in the left atrial appendage and left ventricle in the di-4-ANEPPS-stained rat heart.

Hz pacing (Fig. 2B-b and c). Thus, in principle, cardiomyocytes in the apparently intact atria exhibit spatially coordinated behaviors of intracellular $[Ca^{2+}]_i$ as a functional syncytium.

In contrast to the spatiotemporally uniform $[Ca^{2+}]_i$ dynamics shown above, the rest of the hearts were spatially non-uniform. As shown in the representative X-t images of six different myocytes within an area of imaging in Figure 3a, the apparent spatial uniformity of Ca^{2+} transients during 1-Hz pacing was impaired during higher frequency of excitation at 4 Hz; individual myocytes often failed to evoke Ca^{2+} transients, or instead, exhibited localized rises of $[Ca^{2+}]_i$, which propagated along the longitudinal axis of the individual myocytes, i.e., Ca^{2+} waves. Close representation of the X-t images in extended timescale (Fig. 3b) revealed that wavefronts of the Ca^{2+} transients were apparently regular at 1 Hz, whereas they became irregular and non-uniformity of $[Ca^{2+}]_i$ dynamics was evident in the plot profiles (Fig. 3c). During 4-Hz pacing, while individual myocytes showed complex patterns of fluo-4 fluorescence changes, overall atrial region of observation revealed regular alternans of the amplitude of Ca^{2+} transients in terms of its fluorescence profiles (Fig. 3c). In comparison of the configurations of Ca^{2+} transients in the atria showing uniform dynamics with those showing non-uniform dynamics, the durations were longer during 2- and 3-Hz pacing (Fig. 4a), and the pacing-frequency dependence was more obvious for beat-to-beat variability of the duration and amplitude of the Ca^{2+} transient in the atria (Fig. 4b and 4c).

To address the cause of spatiotemporal inhomogeneity of atrial $[Ca^{2+}]_i$ dynamics, we visualized sequential changes in the fluo-4 fluorescence of the atria showing spatial non-uniformity (Fig. 5). After a long period (~5 s) of quiescence, the pacing-evoked $[Ca^{2+}]_i$ rises were sequentially altered: the first pacing evoked a large amplitude of Ca^{2+} transient with irregular wavefronts that was composed of a mixture of several Ca^{2+} waves. The following pacing showed failure of excitation and occasional emergence of wave-like propagation of $[Ca^{2+}]_i$ rises on systole (i.e., systolic Ca^{2+} waves) with less rapid propagation velocity than those at the initial beat, as evidenced by the less steep decline (i.e., lower propagation velocity), of the waves. Similar observations were obtained in the two other hearts that were examined.

The pacing-induced inhomogeneous $[Ca^{2+}]_i$ dynamics barely accompanied spontaneous rise of $[Ca^{2+}]_i$ during diastole, e.g., diastolic Ca^{2+} waves (Fig. 6). While the atria exhibited beat-to-beat alternans of Ca^{2+} transients during the 5-Hz rapid pacing, they showed no discernible rise of $[Ca^{2+}]_i$ after cessation of the burst pacing. Such minor emergence of spontaneous Ca^{2+} waves was confirmed in all the three atria examined.

IV. Discussion

In the present study we visualized precise $[Ca^{2+}]_i$ dynamics of atrial myocytes in the perfused rat heart. By using the innovative *in situ* rapid confocal imaging system we constructed, we found that atrial appendage in Langendorff-perfused rat heart has a propensity to show spatiotemporally non-uniform $[Ca^{2+}]_i$ dynamics on systole especially during high-frequency excitation. According to our $[Ca^{2+}]_i$ dynamics studies to date [9, 11, 25], such non-uniformity in the Ca^{2+} transients was not predominantly observed in intact ventricles, and the observed features in the atrial $[Ca^{2+}]_i$ dynamics would partly be related to the structural difference, i.e., paucity of t-tubules.

In principle, individual atrial myocytes in the perfused hearts showed spatiotemporally uniform $[Ca^{2+}]_i$ dynamics with frequency-dependent abbreviation of Ca^{2+}-transient durations, a confirmation of the atria being a functional syncytium (Fig. 2). However, even under apparently intact Langendorff perfusion, individual myocytes often exhibited spatially non-uniform $[Ca^{2+}]_i$ dynamics, e.g., cluster-like rises of $[Ca^{2+}]_i$, wave-like propagation of $[Ca^{2+}]_i$, and beat-to-beat variability of durations and amplitude alternans of Ca^{2+} transients, all of which emerged on excitation instead of uniform Ca^{2+} transients (Figs. 3 and 4). The two distinct groups of the atria in this study were categorized not under consideration of specific cause of non-uniformity, but only based on spatial uniformity in $[Ca^{2+}]_i$ dynamics as a matter of practical convenience. However, as compared with the atria showing spatially uniform Ca^{2+} transients, those with inhomogeneous $[Ca^{2+}]_i$ dynamics showed relatively longer duration of Ca^{2+} transients (Fig. 4a). This indicates that $[Ca^{2+}]_i$ handlings in the atria showing non-uniformity can be impaired, especially in the function of the SERCA pump, a crucial Ca^{2+}-ATPase to reuptake Ca^{2+} into the SR,

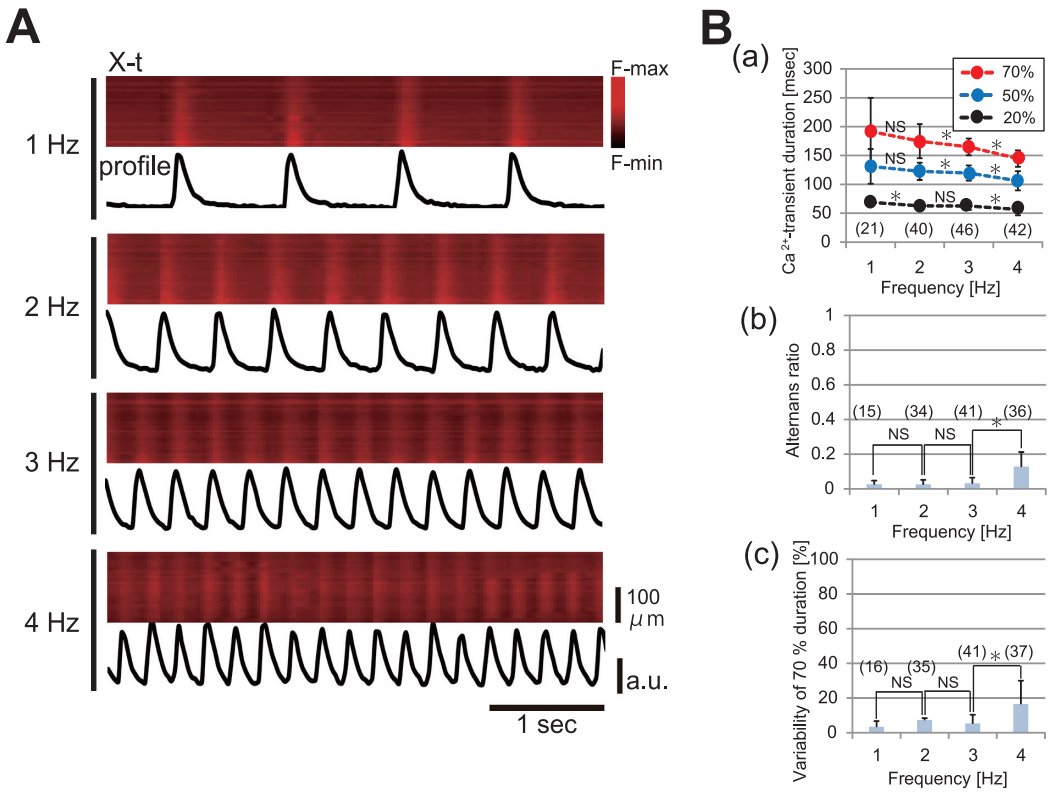

Fig. 2. Properties of the spatially uniform Ca^{2+} transients in the left atria. (**A**) Representative X-t images of the fluo-4 fluorescence intensity and the corresponding plot profiles of individual atrial myocytes in the left atrial appendage under pacing at 1–4 Hz. (**B**) Quantitative data of Ca^{2+} transients. (**a**) Pacing-frequency dependence of the durations at 20%-, 50%-, and 70%-amplitudes. The * and NS shown between the circles denote the statistical results for the Ca^{2+}-transient durations evaluated between the two different adjacent frequencies at the same level. (**b**) Beat-to-beat variability of the Ca^{2+} alternans ratio, i.e., relative values of the changes in the amplitude over the previous Ca^{2+}-transient amplitude plotted against the frequency of pacing. (**c**) Beat-to-beat variability of the Ca^{2+} transient duration at 70%. Percent values of the changes in the duration over the mean duration of the Ca^{2+} transients plotted against the frequency of pacing. Numbers in parentheses denote the numbers in Ca^{2+} transients analyzed from 5 hearts. * denotes $p<0.05$. NS, no significant difference.

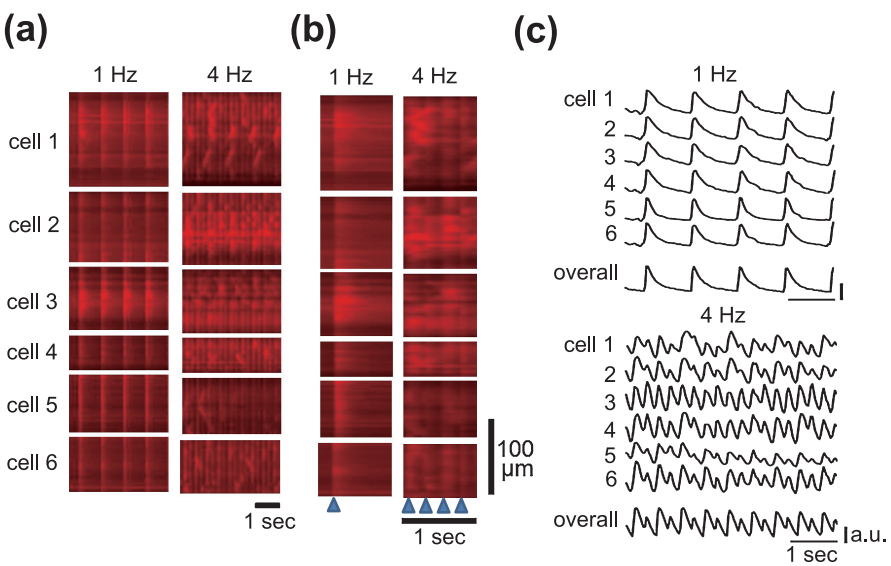

Fig. 3. Pacing frequency-dependent non-uniformity of Ca^{2+} transients in the left atria. (**a**) Representative X-t images of Ca^{2+} transients in six different myocytes (cell 1–cell 6) in the left atrial appendage during pacing at 1 Hz (left) and 4-Hz (right). (**b**) Comparison of the wavefronts of Ca^{2+} transients in (**a**) shown in expanded time scale. Blue arrowheads on the bottom denote the timing of pacing. (**c**) Corresponding plot profiles of X-t images, and mean plot profiles of the overall atrial region imaged.

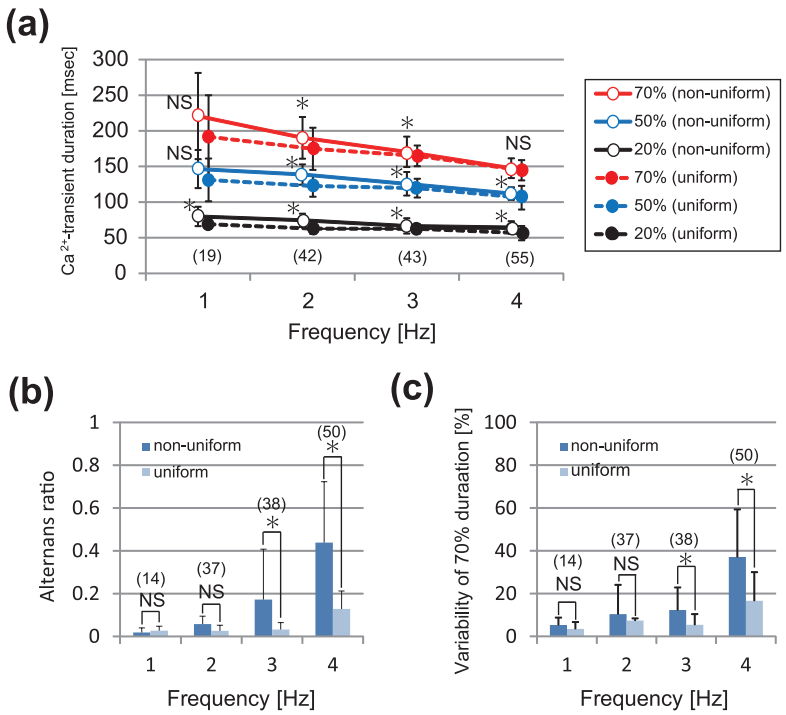

Fig. 4. Pacing-frequency dependence of (**a**) the durations at 20%-, 50%-, and 70%-amplitudes, (**b**) alternans ratio, and (**c**) variability of Ca^{2+} transient duration at 70% decay in the atria showing non-uniform Ca^{2+} transients. The data for the atria showing uniform Ca^{2+} transients (shown in Figure 2B) are also added to the graphs. In (**a**) statistical significance was evaluated between the 'uniform Ca^{2+} transients' group shown in Figure 2B and 'non-uniform Ca^{2+} transients' group. Numbers in parentheses denote the numbers in Ca^{2+} transients analyzed from 5 hearts. * denotes $p<0.05$. NS, no significant difference.

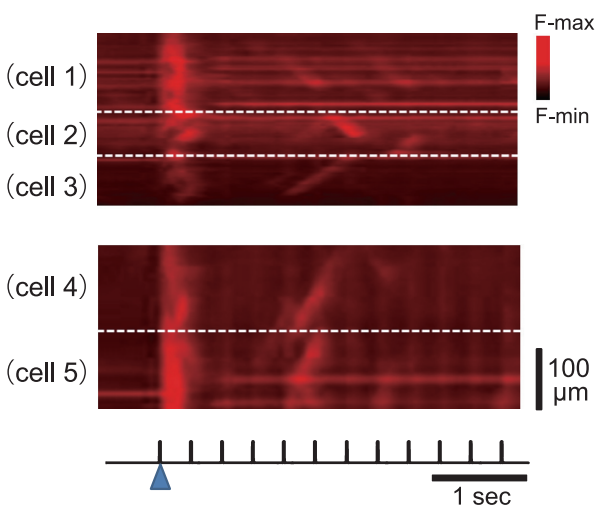

Fig. 5. Sequential changes in the pacing-evoked Ca^{2+} transients after quiescence. Two representative X-t images of the left atrial myocytes. Each X-t image obtained from the region consisted of 2–3 cells as delineated by broken lines. Electrical stimuli are shown on the bottom. The blue arrowhead denotes the time point of the initial pacing.

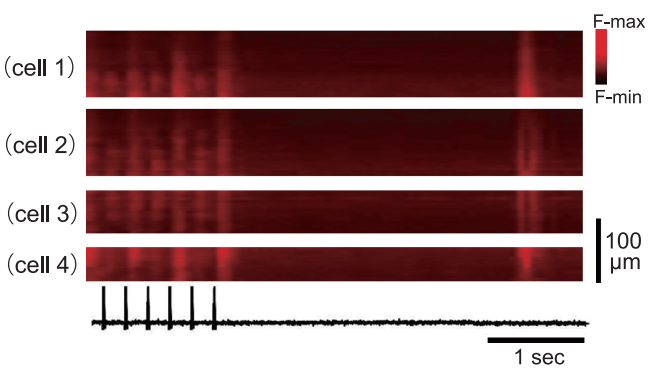

Fig. 6. Absence of the spontaneous Ca^{2+} waves after burst pacing of the left atrium showing beat-to-beat Ca^{2+} alternans. X-t images of four different cells. Electrical stimuli are shown on the bottom. Six non-uniform Ca^{2+} transients were evoked by burst pacing at 5 Hz. About 300 milliseconds after pacing, one spontaneous Ca^{2+} transient occurred showing relatively uniform wavefronts for individual cells.

which may well occur under metabolic inhibition [8]. In the present experiments, certain degrees of metabolic inhibition may have occurred due to, e.g., indeterminable poor coronary-arterial perfusion in the atria or long-term (~10 min) placement on the atria of a glass coverslip during confocal imaging ('coverslip hypoxia' [19]). The non-uniform $[Ca^{2+}]_i$ dynamics observed here may also be a consequence of metabolic inhibition and the resultant depression of Ca^{2+} release from the SR. This possibility is evidenced by the previous studies on isolated atrial myocytes, where similar non-uniform $[Ca^{2+}]_i$ dynamics occurred in isolated atrial and ventricular myocytes due to metabolic inhibition or acidosis [7, 14].

The non-uniform $[Ca^{2+}]_i$ dynamics we identified in the atria included Ca^{2+} waves that emerge on systole, which are in stark contrast to the well-known diastolic Ca^{2+} waves

caused by $[Ca^{2+}]_i$ overload [22, 24]. The sequential changes in the $[Ca^{2+}]_i$ dynamics evoked after a period of quiescence (Fig. 5) indicate a possible mechanism for the systolic Ca^{2+} waves. Emergence of the slowly propagating waves following the initial Ca^{2+} transient composed of several wave-like clusters of $[Ca^{2+}]_i$ rise indicates a progressive decrease in the amount of Ca^{2+} release from the SR. It is therefore likely that the systolic Ca^{2+} waves are caused not by $[Ca^{2+}]_i$ overload, but by impairment of Ca^{2+} release from the SR or accumulation of a small amount of Ca^{2+} in the SR. Absence of the definitive $[Ca^{2+}]_i$ overload in the atria studied here was also supported by the observation of $[Ca^{2+}]_i$ after cessation of burst pacing (Fig. 6).

The structural differences in t-tubular distribution between the atrial myocytes and the ventricular cells we confirmed here in cardiac tissues (Fig. 1) may also account for the propensity of the atrial cells to show non-uniform $[Ca^{2+}]_i$ dynamics. In atrial myocytes devoid of t-tubules, $[Ca^{2+}]_i$ rises evoked on excitation would be originated solely from influx of Ca^{2+} from Ca^{2+} channels on surface sarcolemmal membranes [5], whereas ventricular cells are much more efficient for providing Ca^{2+} to evoke uniform Ca^{2+} transients because of the abundant invagination of t-tubules. Considering the crucial role of t-tubules in uniformity of $[Ca^{2+}]_i$ dynamics, atrial myocytes are less efficient at exhibiting Ca^{2+} transients throughout the entire region of the cells than ventricular cells, and thereby, have a propensity to show non-uniform $[Ca^{2+}]_i$ dynamics [5].

Compared with the intact atrial myocytes, in which t-tubules are abundantly distributed, those obtained from sheep with persistent atrial fibrillation reportedly show significant reduction of t-tubular networks and non-uniform wavefronts of Ca^{2+} transients [15]. This is in good agreement with our present observations that decrease in the tubular networks results in spatial non-uniformity of $[Ca^{2+}]_i$ dynamics. Depressed distribution of the t-tubular network was also reported in ventricular myocytes in certain diseased states, e.g., failing hearts or remodeled heart after myocardial infarct, where again $[Ca^{2+}]_i$ dynamics show spatiotemporal inhomogeneity [3, 16, 17]. In combination, it is likely that depressed, disorganized distribution of t-tubules caused by diseased states is important in generation of non-uniform $[Ca^{2+}]_i$ dynamics in the heart.

We should note limitations of this study. First, we observed the $[Ca^{2+}]_i$ dynamics under perfusion at room temperature. Second, contribution of sympathetic modulation was not considered because the hearts were excised. These factors may well promote inhomogeneity of $[Ca^{2+}]_i$ dynamics. Therefore, our observations may not necessarily be relevant to the atrial $[Ca^{2+}]_i$ dynamics that arise under physiological conditions *in situ*. Nevertheless, the propensity to the impaired $[Ca^{2+}]_i$ dynamics we observed here would hold true, and therefore, the $[Ca^{2+}]_i$ non-uniformity would more or less arise in diseased states of the atria, e.g., during persisting atrial fibrillation, ischemia and metabolic inhibition. In the future it should be clarified whether and how spatially non-uniform $[Ca^{2+}]_i$ dynamics really arise within the atria in diseased hearts and contribute to contractile failure and generation of tachyarrhythmias.

V. Disclosures

None.

VI. Acknowledgment

This work was supported by a Grant-in-Aid for Scientific Research (C, 24590487) from the Ministry of Education, Culture, Sports, Science and Technology of Japan.

VII. References

1. Aistrup, G. L., Kelly, J. E., Kapur, S., Kowalczyk, M., Sysman-Wolpin, I., Kadish, A. H. and Wasserstrom, J. A. (2006) Pacing-induced heterogeneities in intracellular Ca^{2+} signaling, cardiac alternans, and ventricular arrhythmias in intact rat heart. *Circ. Res.* 99; e65–e73.
2. Ayettey, A. S. and Navaratnam, V. (1978) The T-tubule system in the specialized and general myocardium of the rat. *J. Anat.* 127; 125–140.
3. Balijepalli, R. C., Lokuta, A. J., Maertz, N. A., Buck, J. M., Haworth, R. A., Valdiviab, H. H. and Kampa, T. J. (2003) Depletion of T-tubules and specific subcellular changes in sarcolemmal proteins in tachycardia-induced heart failure. *Cardiovasc. Res.* 59; 67–77.
4. Bers, D. M. (2002) Cardiac excitation-contraction coupling. *Nature* 415; 198–205.
5. Bootman, M. D., Higazi, D. R., Coombes, S. and Roderick, H. L. (2006) Calcium signalling during excitation-contraction coupling in mammalian atrial myocytes. *J. Cell Sci.* 119; 3915–3925.
6. Cheng, H., Lederer, W. J. and Cannell, M. B. (1993) Calcium sparks: elementary events underlying excitation-contraction coupling in heart muscle. *Science* 262; 740–744.
7. Díaz, M. E., Eisner, D. A. and O'Neill, S. C. (2002) Depressed ryanodine receptor activity increases variability and duration of the systolic Ca^{2+} transient in rat ventricular myocytes. *Circ. Res.* 91; 585–593.
8. Eisner, D., Bode, E., Venetucci, L. and Trafford, A. (2013) Calcium flux balance in the heart. *J. Mol. Cell. Cardiol.* 58; 110–117.
9. Fujiwara, K., Tanaka, H., Mani, H., Nakagami, T. and Takamatsu, T. (2008) Burst emergence of intracellular Ca^{2+} waves evokes arrhythmogenic oscillatory depolarization via the Na+-Ca^{2+} exchanger: simultaneous confocal recording of membrane potential and intracellular Ca^{2+} in the heart. *Circ. Res.* 103; 509–518.
10. Hama, T., Takahashi, A., Ichihara, A. and Takamatsu, T. (1998) Real time in situ confocal imaging of calcium wave in the perfused whole heart of the rat. *Cell. Signal.* 10; 331–337.
11. Hamamoto, T., Tanaka, H., Mani, H., Tanabe, T., Fujiwara, K., Nakagami, T., Horie, M., Oyamada, M. and Takamatsu, T. (2005) In situ Ca^{2+} dynamics of Purkinje fibers and its interconnection with subjacent ventricular myocytes. *J. Mol. Cell. Cardiol.* 38; 561–569.
12. Kaneko, T., Tanaka, H., Oyamada, M., Kawata, S. and Takamatsu, T. (2000) Three distinct types of Ca^{2+} waves in Langendorff-perfused rat heart revealed by real-time confocal microscopy. *Circ. Res.* 86; 1093–1099.
13. Kapur, S., Wasserstrom, J. A., Kelly, J. E., Kadish, A. H. and

Aistrup, G. L. (2009) Acidosis and ischemia increase cellular Ca^{2+} transient alternans and repolarization alternans susceptibility in the intact rat heart. *Am. J. Physiol. Heart Circ. Physiol.* 296; H1491–H1512.
14. Kockskämper, J., Zima, A. V. and Blatter, L. A. (2005) Modulation of sarcoplasmic reticulum Ca^{2+} release by glycolysis in cat atrial myocytes. *J. Physiol.* 564; 697–714.
15. Lenaerts, I., Bito, V., Heinzel, F. R., Driesen, R. B., Holemans, P., D'hooge, J., Heidbüchel, H., Sipido, K. R. and Willems, R. (2009) Ultrastructural and functional remodeling of the coupling between Ca^{2+} influx and sarcoplasmic reticulum Ca^{2+} release in right atrial myocytes from experimental and persistent atrial fibrillation. *Circ. Res.* 105; 876–885.
16. Louch, W. E., Bitoa, V., Heinzela, F. R., Macianskienec, R., Vanhaeckea, J., Flamengc, W., Mubagwa, K. and Sipido, K. R. (2004) Reduced synchrony of Ca^{2+} release with loss of T-tubules —a comparison to Ca^{2+} release in human failing cardiomyocytes. *Cardiovasc. Res.* 62; 63–73.
17. Louch, W. E., Mørk, H. K., Sexton, J., Strømme, T. A., Laake, P., Sjaastad, I. and Sejersted, O. M. (2006) T-tubule disorganization and reduced synchrony of Ca^{2+} release in murine cardiomyocytes following myocardial infarction. *J. Physiol.* 574; 519–533.
18. Minamikawa, T., Cody, S. H. and Williams, D. A. (1997) In situ visualization of spontaneous calcium waves within perfused whole rat heart by confocal imaging. *Am. J. Physiol.* 272; H236–H243.
19. Pitts, K. R. and Toombs, C. F. (2004) Coverslip hypoxia: a novel method for studying cardiac myocyte hypoxia and ischemia in vitro. *Am. J. Physiol. Heart Circ. Physiol.* 287; H1801–1812.
20. Rubart, M., Wang, E., Dunn, K. W. and Field, L. J. (2003) Two-photon molecular excitation imaging of Ca^{2+} transients in Langendorff-perfused mouse hearts. *Am. J. Physiol. Cell Physiol.* 284; C1654–C1668.
21. Smyrniasa, I., Maira, W., Harzheima, D., Walkera, S. A., Rodericka, H. L. and Bootman, M. D. (2010) Comparison of the T-tubule system in adult rat ventricular and atrial myocytes and its role in excitation–contraction coupling and inotropic stimulation. *Cell Calcium* 47; 210–223.
22. Takamatsu, T. and Wier, W. G. (1990) Calcium waves in mammalian heart: quantification of origin, magnitude, waveform and velocity. *FASEB J.* 4; 1519–1525.
23. Tanaka, H., Oyamada, M., Tsujii, E., Nakajo, T. and Takamatsu, T. (2002) Excitation-dependent intracellular Ca^{2+} waves at the border zone of the cryo-injured rat heart revealed by real-time confocal microscopy. *J. Mol. Cell. Cardiol.* 34; 1501–1512.
24. Tanaka, H. and Takamatsu, T. (2003) Spatiotemporal visualization of intracellular Ca^{2+} in living heart muscle cells viewed by confocal laserscanning microscopy. *Acta Histochem. Cytochem.* 36; 193–204.
25. Tanaka, H., Hamamoto, T. and Takamatsu, T. (2005) Toward an integrated understanding of the Purkinje fibers in the heart: the functional and morphological interconnection between the Purkinje fibers and ventricular muscle. *Acta Histochem. Cytochem.* 38; 257–265.
26. Xie, W., Santulli, G., Guo, X., Gao, M., Chen, B. X. and Marks, A. R. (2013) Imaging atrial arrhythmic intracellular calcium in intact heart. *J. Mol. Cell. Cardiol.* 64; 120–123.